



# CHALMERS

## Chalmers Publication Library

### **New prompt spectral gamma-ray data from the reaction Cf-252(sf) and its implication on present evaluated nuclear data files**

This document has been downloaded from Chalmers Publication Library (CPL). It is the author's version of a work that was accepted for publication in:

**Physical Review C. Nuclear Physics (ISSN: 0556-2813)**

Citation for the published paper:

Billnert, R. ; Hamsch, F. ; Oberstedt, A. (2013) "New prompt spectral gamma-ray data from the reaction Cf-252(sf) and its implication on present evaluated nuclear data files". Physical Review C. Nuclear Physics, vol. 87(2),

<http://dx.doi.org/10.1103/PhysRevC.87.024601>

Downloaded from: <http://publications.lib.chalmers.se/publication/175151>

Notice: Changes introduced as a result of publishing processes such as copy-editing and formatting may not be reflected in this document. For a definitive version of this work, please refer to the published source. Please note that access to the published version might require a subscription.

Chalmers Publication Library (CPL) offers the possibility of retrieving research publications produced at Chalmers University of Technology. It covers all types of publications: articles, dissertations, licentiate theses, masters theses, conference papers, reports etc. Since 2006 it is the official tool for Chalmers official publication statistics. To ensure that Chalmers research results are disseminated as widely as possible, an Open Access Policy has been adopted. The CPL service is administrated and maintained by Chalmers Library.

(article starts on next page)

# New prompt spectral $\gamma$ -ray data from the reaction $^{252}\text{Cf}(\text{sf})$ and its implication on present evaluated nuclear data files

R. Billnert,<sup>1,2</sup> F.-J. Hamsch,<sup>1</sup> A. Oberstedt,<sup>2,\*</sup> and S. Oberstedt<sup>1,†</sup>

<sup>1</sup>European Commission, Joint Research Centre (IRMM), B-2440 Geel, Belgium

<sup>2</sup>Fundamental Fysik, Chalmers Tekniska Högskola, S-41296 Göteborg, Sweden

(Received 21 September 2012; revised manuscript received 17 January 2013; published 4 February 2013)

We present results from new spectral prompt  $\gamma$ -ray measurements from the spontaneous fission of  $^{252}\text{Cf}$ . Apart from one recent experiment, about four decades have passed since the last dedicated experiments were reported in the literature. Hence, there was a need for a revision. We have measured prompt fission  $\gamma$  rays with both cerium-doped  $\text{LaBr}_3$  and  $\text{CeBr}_3$  scintillation detectors, both of which exhibit excellent timing and good energy resolution. The emission yield was determined to be  $\nu_\gamma = (8.30 \pm 0.08)/\text{fission}$  and  $\nu_\gamma = (8.31 \pm 0.10)/\text{fission}$ , with the average energy of  $\epsilon_\gamma = (0.80 \pm 0.01)$  MeV and  $\epsilon_\gamma = (0.80 \pm 0.01)$  MeV and total energy of  $E_{\gamma,\text{tot}} = (6.64 \pm 0.08)$  MeV and  $E_{\gamma,\text{tot}} = (6.65 \pm 0.12)$  MeV, with the  $\text{LaBr}_3$  and  $\text{CeBr}_3$  detectors, respectively. Since the results from the two detectors are in excellent agreement and confirm the historical data, but not those in the present evaluated nuclear data files, we strongly recommend an update.

DOI: [10.1103/PhysRevC.87.024601](https://doi.org/10.1103/PhysRevC.87.024601)

PACS number(s): 07.85.Nc, 24.75.+i, 25.85.Ca, 29.30.Kv

## I. INTRODUCTION

With the potential of more advanced nuclear reactors in the near future, a better understanding of the entire fission process is needed. Since four out of six of the impending Generation-IV reactors that have been selected by the Generation-IV International Forum (GIF) are fast reactors, an innovative core design is required to be able to handle the excessive heat deposit from the fission process [1]. In order to model these cores, a better understanding of the released heat from the common reactor isotopes is crucial. Present knowledge regarding this heat deposit implies that approximately 10% of the total energy released in fission is due to  $\gamma$  rays, of which around 40% of the heat originates from prompt fission  $\gamma$  rays [2]. According to Refs. [1,3] it is necessary to achieve an uncertainty of at most 7.5% with respect to the calculated  $\gamma$  heating in order to adequately model these cores. However, with evaluated data the  $\gamma$  heating is underestimated by up to 28% for the main reactor isotopes  $^{235}\text{U}(n, f)$  and  $^{239}\text{Pu}(n, f)$ . Therefore, these two isotopes have been included in the OECD Nuclear Energy Agency high-priority request list for prompt fission  $\gamma$ -ray data; in particular new values for  $\gamma$  multiplicity and mean energy [4] are requested. The data in the evaluated data tables for both isotopes rely on results that were measured in the early 1970s [5,6] and were recently confirmed by Kwan *et al.* [7]. Hence, it might be more likely that the underestimation comes from the isotopes  $^{238}\text{U}(n, f)$  and  $^{241}\text{Pu}(n, f)$ , which are always produced in a reactor [8]. The evaluated data for those two isotopes exhibit exactly the same structure, with an individual scaling factor; and the same formula is also used for  $^{252}\text{Cf}$ . Accordingly, it seems that no experimental data have been used to evaluate any of these three isotopes. Since the 1970s significant advances have occurred

in detector development, especially with the release of new lanthanide-halide scintillation detectors [9–24], as well as new data acquisition and signal-processing techniques [25,26]. Consequently, we wanted to take advantage of these advancements toward high-quality measurements of the  $\gamma$ -decay heat from the fission process. To make an independent verification of the historical data, we performed an experiment on prompt  $\gamma$  rays from neutron-induced fission of  $^{235}\text{U}$ , and we also plan an identical measurement on  $^{241}\text{Pu}$ , in order to investigate whether this isotope is the source of the underestimation mentioned above. To be able to accurately measure these isotopes we need to be certain of the quality of our experimental setup. Therefore, we started by studying the spontaneous fission of  $^{252}\text{Cf}$ . Since this reaction has been measured both in the early 1970s by Verbinski *et al.* [5] and Pleasonton *et al.* [6], as well as very recently by Chyzh *et al.* with the DANCE spectrometer at Los Alamos National Laboratory [27], it serves as excellent proof of principle. The spectral data from our recent measurement are presented in this work.

## II. CHOICE OF SUITABLE $\gamma$ -RAY DETECTORS

In order to minimize the uncertainty in determining  $\gamma$ -ray multiplicity and mean energy, three important detector characteristics ought to be considered: (1) energy resolution, in order to be able to determine the structure of the emission spectra with good precision, (2) intrinsic full peak efficiency, in order to decrease the uncertainty of the response function, and (3) timing resolution, in order to efficiently separate prompt fission  $\gamma$  rays from prompt fast neutrons by means of time of flight. The new lanthanide-halide scintillation detectors promise to provide a good compromise among these three properties. Therefore, at the Institute for Reference Materials and Measurements (IRMM) we purchased three different scintillation detector types, based on cerium-doped lanthanum-chloride ( $\text{LaCl}_3:\text{Ce}$ ), cerium-doped lanthanum-bromide ( $\text{LaBr}_3:\text{Ce}$ ), and cerium-bromide ( $\text{CeBr}_3$ ) crystals, respectively. After their

\*Present address: CEA/DAM, Ile-de-France, F-91297 Arpajon Cedex, France.

†Corresponding author: [stephan.oberstedt@ec.europa.eu](mailto:stephan.oberstedt@ec.europa.eu)

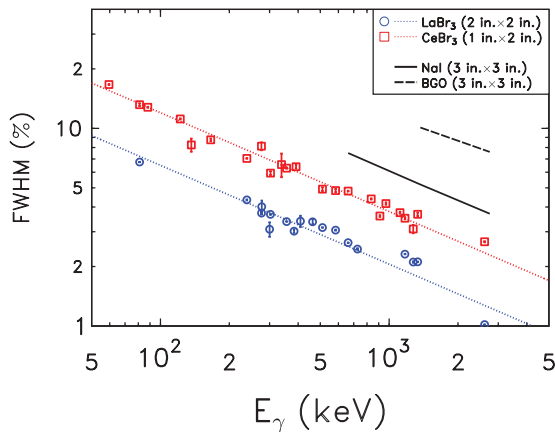


FIG. 1. (Color online) Energy resolution (FWHM) in percent as a function of  $\gamma$ -ray energy for a 2 in.  $\times$  2 in.  $\text{LaBr}_3\text{:Ce}$  detector (circles) and a 1 in.  $\times$  2 in.  $\text{CeBr}_3$  detector (squares); the data are compared to a standard NaI detector as well as a BGO detectors [30].

extensive characterization, using different calibration sources with  $\gamma$ -ray energies between 81 keV ( $^{133}\text{Ba}$ ) up to 2.6 MeV ( $^{232}\text{Th}$  decay series), we decided to use lanthanum-bromide, because of its superior timing as well as energy resolution [23], and cerium-bromide, for its absence of intrinsic activity [24,28]. In previous measurements on prompt fission  $\gamma$  rays [5,6], sodium-iodine (NaI) detectors were used to investigate the  $\gamma$  multiplicity and mean energy. Therefore it was important for us to know how our detectors compare to a typical sodium-iodine detector. As shown in Fig. 1, the energy resolutions, defined as the full width at half maximum (FWHM) in percent, of a 1 in.  $\times$  2 in.  $\text{CeBr}_3$  detector and a 2 in.  $\times$  2 in.  $\text{LaBr}_3\text{:Ce}$  detector are around 2/3 and 2/5, respectively, of that of a 3 in.  $\times$  3 in. NaI detector [30]. For comparison, data for a 3 in.  $\times$  3 in. bismuth germanium oxide (BGO) detector [30] is depicted, too. With respect to intrinsic peak efficiency (Fig. 2), both lanthanide-bromide detectors are about twice as good

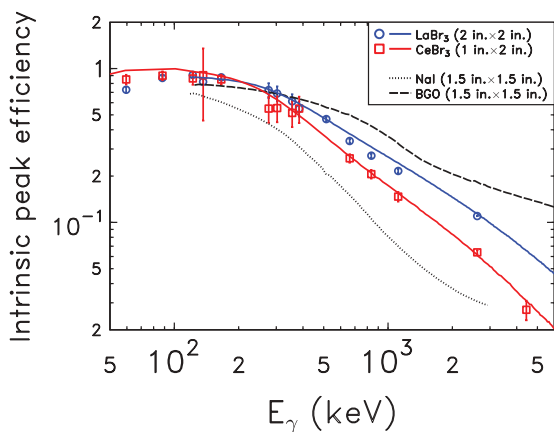


FIG. 2. (Color online) Intrinsic peak efficiency as a function of  $\gamma$ -ray energy for a 2 in.  $\times$  2 in. large  $\text{LaBr}_3\text{:Ce}$  detector (circles) and a 1 in.  $\times$  2 in.  $\text{CeBr}_3$  detector (squares) together with the corresponding results from Monte Carlo simulations (full lines). For comparison the efficiency of both a NaI detector (dotted line) and a BGO detector (dashed line), both of size 1.5 in.  $\times$  1.5 in., are shown as well [30].

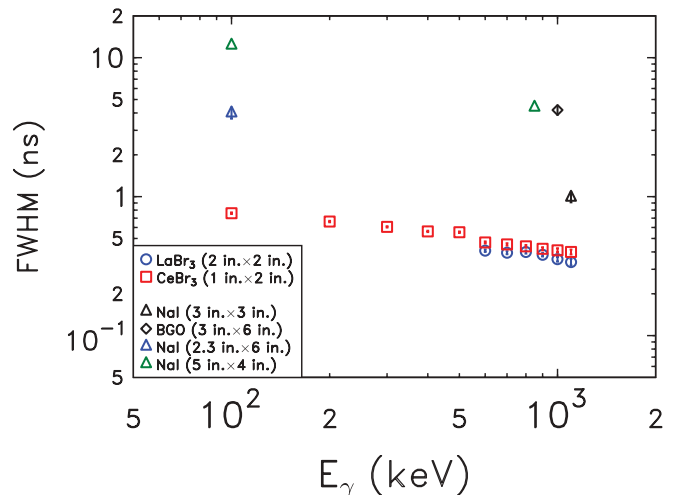


FIG. 3. (Color online) Timing resolution (FWHM) as a function of  $\gamma$ -ray energy for a 2 in.  $\times$  2 in.  $\text{LaBr}_3\text{:Ce}$  detector (circles) and a 1 in.  $\times$  2 in.  $\text{CeBr}_3$  detector (squares); see text for details. For comparison the timing resolution for different NaI and BGO detectors, used in previous studies for spectral measurements, is shown as well [5,6,30].

as a 1.5 in.  $\times$  1.5 in. NaI detector [30] but only around two thirds as good as a 1.5 in.  $\times$  1.5 in. BGO detector [30]. For the experimental determination of the intrinsic peak efficiency we included also  $^{241}\text{Am}$  ( $E_\gamma = 60$  keV) and the reaction  $^{241}\text{Am}(\alpha, n)^9\text{Be}$  ( $E_\gamma = 4.4$  MeV). In addition, we performed Monte Carlo simulations with the code PENELOPE [31]; these simulations fit very well the experimental data, as shown with different full lines in Fig. 2. The last property we needed to consider is timing resolution (Fig. 3). Here we wanted to investigate the timing resolution relative to the energy of the incoming particle, so we measured with different calibration sources ( $^{22}\text{Na}$  or  $^{60}\text{Co}$ ) and applied certain energy thresholds. The measurements were carried out in coincidence with a previously characterized  $\text{LaCl}_3$  detector [29]. Even though we do not have any comparable data for the other detectors regarding different thresholds, we can still see that both the  $\text{CeBr}_3$  and the  $\text{LaBr}_3\text{:Ce}$  detectors are much faster than either the NaI and or the BGO detector [5,6,30]. Of course, we may keep in mind that the  $\text{BaF}_3$  detectors used in Ref. [27] possess an even better timing resolution than lanthanide-halide detectors. However, with an energy resolution well inferior to that of NaI, we do not consider such a detector as useful for our later extended correlated measurements of prompt fission  $\gamma$  rays and fission-fragment properties.

### III. PROMPT FISSION $\gamma$ -RAY SETUP

In order to separate prompt fission  $\gamma$  rays from neutron-induced  $\gamma$  rays, we employed the time-of-flight method. This technique requires a fission trigger, which was provided by a simplified ionization chamber (IC) loaded with a  $^{252}\text{Cf}$  source. The IC was built from very thin walls, i.e., 0.2 mm, to minimize the  $\gamma$ -ray background due to interaction with prompt fission neutrons and operated with P10 gas (a mixture of 90% Ar

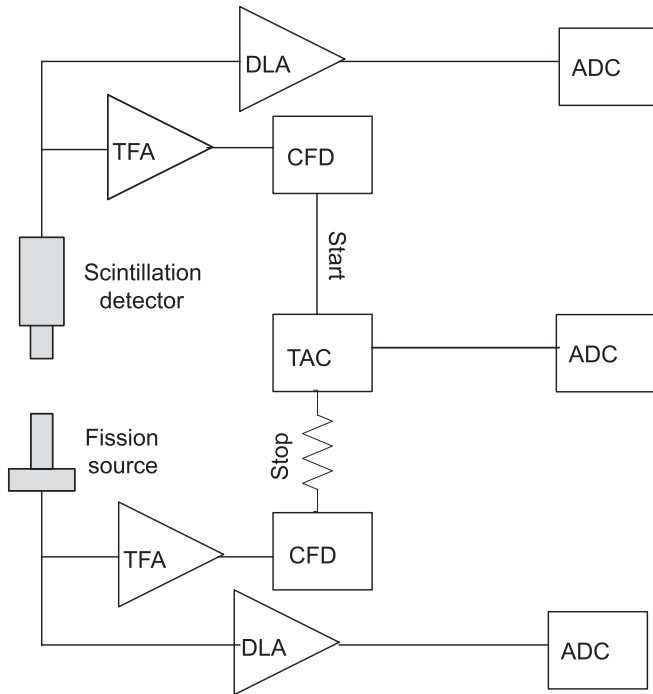


FIG. 4. Experimental setup with an ionization chamber containing a  $^{252}\text{Cf}$  source, which had a source strength of  $8600 \pm 100$  fissions/s. The distance between the fission source and the  $\gamma$ -ray detector was 63 cm. More details may be found in the text.

and 10%  $\text{CH}_4$ , at  $p = 1.2$  bars) [32]. The californium was deposited on a polished stainless steel disk with a 25-mm diameter. The source distributed on a 10-mm-diameter spot had an activity of  $8600 \pm 100$  fissions/s and was mounted inside on the cathode, giving a signal for every fission event. This signal was fed into a slot of an Ortec 935 quad constant fraction discriminator (CFD) via a timing filter amplifier (TFA) of type Ortec 474, and then with a proper delay into the stop input of a Ortec 567 time-to-amplitude converter (TAC). For the start input we used the scintillation detector, which was placed at a distance of 63 cm from the fission source. The distance between the detector and the source was determined with respect to the specific timing resolution of each detector in combination with the IC, i.e.,  $\sigma_{\text{TOF}} < 1.5$  ns, to make sure that there was a sufficient time difference between the prompt  $\gamma$  peak and the fast neutron interactions. The distance is a compromise to have optimum suppression of the prompt fission neutron component and count rate. The direct signals from both the scintillation detector and the fission trigger chamber were also fed via Ortec 460 delay line amplifiers (DLAs) into Canberra 8715 analog-to-digital converters (ADCs) (cf. Fig. 4). This setup gave us the opportunity to select time windows in order to eliminate all events that arrived later than what we expected from a prompt fission  $\gamma$  ray.

#### IV. SPECTRAL DATA

Once we had measured the prompt fission  $\gamma$ -ray spectra, we needed to unfold them with the corresponding detector's

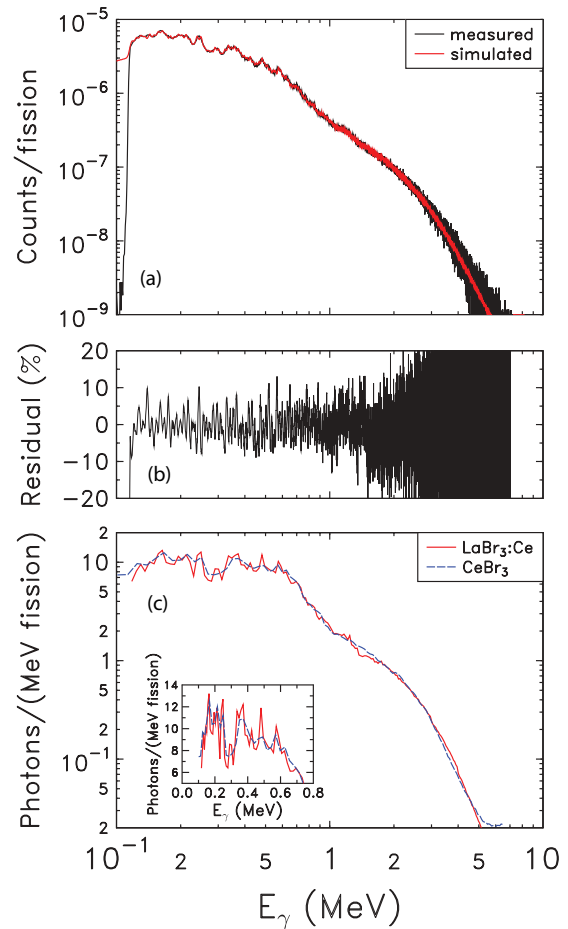


FIG. 5. (Color online) (a) The integral simulated spectrum (red line) adjusted to the experimental one (black line) from the measurement with a 2 in.  $\times$  2 in.  $\text{LaBr}_3\text{:Ce}$  detector. (b) The relative difference between the measured spectrum and the simulation. (c) The unfolded prompt fission  $\gamma$ -ray emission spectrum taken with a 2 in.  $\times$  2 in.  $\text{LaBr}_3\text{:Ce}$  detector (full red line) and a 1 in.  $\times$  2 in.  $\text{CeBr}_3$  detector (dashed blue line). The inset focuses on  $\gamma$ -ray energies below 1 MeV and demonstrates the very good agreement between the results obtained with the two detectors used in this work.

response function in order to determine the emission spectra from the source. These integral response functions were obtained by simulating the response of 220 different energies using again the Monte Carlo code PENELOPE [31] and folded with the experimentally found energy resolution (cf. Fig. 1). These individual energy spectra were then fitted to the measured prompt fission  $\gamma$ -ray spectra, starting with the highest energy and moving toward the lower ones. From the factor needed to adjust the first simulated energy peak to the measured spectra, we deduced the amount of photons of that particular energy which the source emits in  $4\pi$ . The fully simulated distribution, including Compton continuum and escape peaks (for energies above 1.022 MeV), was then subtracted from the measured spectrum, and the next lower energy was fitted, and so on. The simulated integral response function as well as the corresponding prompt  $\gamma$ -ray spectrum from the measurement with the  $\text{LaBr}_3$  detector can be seen in Fig. 5(a). Figure 5(b) shows the residuals, i.e., the relative deviations between



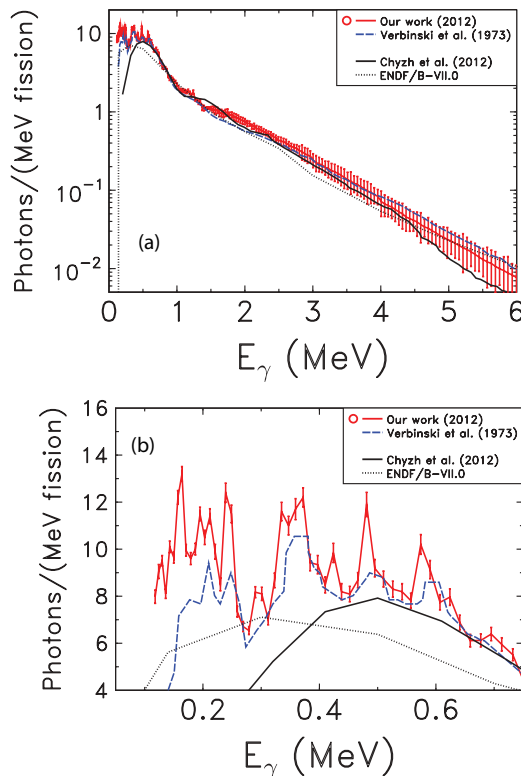


FIG. 6. (Color online) (a) The prompt fission  $\gamma$ -ray emission spectrum from this work taken with a 2 in.  $\times$  2 in. LaBr<sub>3</sub>:Ce detector (full red line) shown together with data from Refs. [5,27] as well as from ENDF/B-VII for comparison. In the high-energy range, all spectra agree rather well with each other, but the data from both ENDF/B-VII.0 [33] and Ref. [27] lack structure in the low-energy range. This is even more obvious in (b), which focuses on  $\gamma$ -ray energies below 0.8 MeV, and demonstrates on the other hand the very good reproduction of the historical data from Ref. [5] (see text for details).

measured and simulated spectra. The overall agreement is obviously good. The unfolded emission spectra from both the LaBr<sub>3</sub>:Ce and the CeBr<sub>3</sub> detector are depicted in Fig. 5(c). Here we notice that the results obtained with the two detectors agree very well with each other, which is impressively obvious also by the low-energy structure shown in the inset. In Fig. 6 we compare our results obtained with the LaBr<sub>3</sub>:Ce detector with those from Verbinski *et al.* [5] and Chyzh *et al.* [27], as well as with the data from the evaluated data tables (ENDF/B-VII.0 [33]) on the reaction  $^{251}\text{Cf}(n_{\text{th}}, f)$ . As can be seen, our data are consistent with the previously measured spectra, but the evaluated data do not describe well any of these experimental data sets. The explanation for this discrepancy is probably that the evaluated data for  $^{252}\text{Cf}^*$  might not be based on any experimental data. In the low-energy region we notice again the previously mentioned structure in the emission spectra, which is similar for all three sets of experimental data, but since the LaBr<sub>3</sub> detector has a superior energy resolution, the structure is more pronounced in the spectrum taken with this detector (cf. also Fig. 5). For integral  $\gamma$  multiplicity and total energy, this energy resolution is not important. However, if we want to further correlate prompt  $\gamma$  emission with certain fission product characteristics, e.g., mass, it is important to

have an energy resolution as good as possible. It should be noted that the error bars for our data contain both statistical uncertainties as well as uncertainties from the determination of the response function. The results that are most relevant for nuclear applications are summarized in Table I. The total  $\gamma$ -ray energy obtained from the ENDF/B-VII.0 evaluated multiplicity and mean  $\gamma$ -ray energy is 15% smaller than the average value calculated from Verbinski's and our work.

## V. CONCLUSION

In this work we have presented the results from our first prompt fission  $\gamma$ -ray spectral measurements of the reaction  $^{252}\text{Cf}(\text{sf})$ . The shapes of the measured spectra from two different detectors agree very well with each other and with previously published ones from the early 1970s [5,6]. The same is true, at least for high  $\gamma$  energies, for recent results of Chyzh *et al.* [27]. The characteristic parameters as listed in Table I are also nicely reproduced, except for the average energy of a  $\gamma$  ray as well as the total  $\gamma$  energy given in Ref. [27]. This discrepancy, however, is understandable, since the detectors from Ref. [27] are not able to efficiently measure the low-energy region due to absorption effects. Hence, both mean and total energy are overestimated. All this gives us confidence that both our method of measuring prompt fission  $\gamma$  rays and the determination of the integral response function of both employed detectors are accurate. Since the data in ENDF/B-VII do not match either our data nor the experimental data from Refs. [5,6,27], we strongly suggest that the evaluated data tables should be updated as soon as possible.

We also noticed that the data in the evaluated tables for  $^{238}\text{U}$  and  $^{241}\text{Pu}$  seem to have been obtained by simply applying a scaling factor to the evaluation for  $^{252}\text{Cf}$ . Since we have shown here that the evaluated data for  $^{252}\text{Cf}$  are in conflict with existing experimental results, it might be reasonable to assume that at least some of the underestimation mentioned by Rimpault *et al.* [1,3] is due to an unrealistic evaluation of prompt fission  $\gamma$ -ray data from  $^{238}\text{U}$  and  $^{241}\text{Pu}$ . In the next

TABLE I. Overview of results for the spontaneous fission of  $^{252}\text{Cf}$ . The experimental results from this work for the prompt fission  $\gamma$ -ray multiplicity  $\nu_\gamma$ , the average energy  $\epsilon_\gamma$ , and the total energy  $E_{\gamma,\text{tot}}$ , obtained with both detectors employed here, are compared to previously measured values from Refs. [5,6,27] as well as corresponding numbers from the evaluated nuclear data files in ENDF/B-VII.0 [33].

Results	$\nu_\gamma$ (per fission)	$\epsilon_\gamma$ (MeV)	$E_{\gamma,\text{tot}}$ (MeV)
This work (LaBr <sub>3</sub> :Ce)	$8.30 \pm 0.08$	$0.80 \pm 0.01$	$6.64 \pm 0.08$
This work (CeBr <sub>3</sub> )	$8.31 \pm 0.10$	$0.80 \pm 0.01$	$6.65 \pm 0.12$
Verbinski <i>et al.</i> [5]	$7.80 \pm 0.30$	$0.88 \pm 0.04$	$6.84 \pm 0.30$
Pleasanton <i>et al.</i> [6]	$8.32 \pm 0.40$	$0.85 \pm 0.06$	$7.06 \pm 0.35$
Chyzh <i>et al.</i> [27]	$8.14 \pm 0.4$	$0.94 \pm 0.05$	$7.65 \pm 0.55$
ENDF/B-VII.0 <sup>a</sup>	7.48	0.76	5.71

<sup>a</sup>During the refereeing process ENDF/B-VII.1 was released, still leading to an underestimation of the total prompt  $\gamma$ -ray energy release by 9%.

step we will analyze our measurement on  $^{235}\text{U}$ , in order to possibly confirm the historical data regarding this isotope, as well as to further investigate correlations between certain  $\gamma$  energies with different fission fragment characteristics for both  $^{235}\text{U}(n_{\text{th}}, f)$  and  $^{252}\text{Cf}(sf)$ .

## ACKNOWLEDGMENTS

One of the authors (R.B.) is indebted to the European Commission for support at the Joint Research Centre IRMM, where this work was carried out.

- 
- [1] G. Rimpault, in *Nuclear Data Needs for Generation IV*, edited by P. Rullhusen (World Scientific, Antwerp, 2006), p. 46.
- [2] K. S. Krane, in *Introductory Nuclear Physics* (Wiley, New York, 1988), p. 493.
- [3] G. Rimpault, A. Courcelle, and D. Blanchet, Comment to the HPRL: ID H.3 and H.4.
- [4] Nuclear Data High Priority Request List of the NEA (Req. ID: H.3, H.4), <http://www.nea.fr/html/dbdata/hprl/hprlview.pl?ID=421> and <http://www.nea.fr/html/dbdata/hprl/hprlview.pl?ID=422>.
- [5] V. V. Verbinski, H. Weber, and R. E. Sund, *Phys. Rev. C* **7**, 1173 (1973).
- [6] F. Pleasonton, R. L. Ferguson, and H. W. Schmitt, *Phys. Rev. C* **6**, 1023 (1972).
- [7] E. Kwan *et al.*, *Nucl. Instrum. Methods A* **688**, 55 (2012).
- [8] O. Sérot (private communication).
- [9] K. Shah, J. Glodo, M. Klugerman, W. W. Moses, S. E. Derenzo, and M. J. Weber, *IEEE Nucl. Sci. Symp. Confer. Rec.* **1**, 92 (2002).
- [10] K. S. Shah, J. Glodo, M. Klugerman, L. Cirignano, W. W. Moses, S. E. Derenzo, and M. J. Weber, *Nucl. Instrum. Methods A* **505**, 76 (2003).
- [11] A. Iltis, M. R. Mayhugh, P. Menge, C. M. Rozsa, O. Selles, and V. Solovyev, *Nucl. Instrum. Methods A* **563**, 359 (2006).
- [12] B. D. Milbrath, B. J. Choate, J. E. Fast, W. K. Hensley, R. T. Kouzes, and J. E. Schweppe, *Nucl. Instrum. Methods A* **572**, 774 (2007).
- [13] A. Owens, A. J. J. Bos, S. Brandeburg, C. Dathy, P. Dorenbos, S. Kraft, R. W. Ostendorf, V. Ouspenski, and F. Quarati, *Nucl. Instrum. Methods A* **574**, 110 (2007).
- [14] F. Quarati, A. J. J. Bos, S. Brandeburg, C. Dathy, P. Dorenbos, S. Kraft, R. W. Ostendorf, V. Ouspenski, and A. Owens, *Nucl. Instrum. Methods A* **574**, 115 (2007).
- [15] R. Nicolini *et al.*, *Nucl. Instrum. Methods A* **582**, 554 (2007).
- [16] P. R. Menge, G. Gautier, A. Iltis, C. Rozsa, and V. Solovyev, *Nucl. Instrum. Methods A* **579**, 6 (2007).
- [17] B. Ayaz-Maierhafer and T. A. DeVol, *Nucl. Instrum. Methods A* **579**, 410 (2007).
- [18] A. Favalli, H.-C. Mehner, and F. Simonelli, *Radiat. Meas.* **43**, 506 (2008).
- [19] M. Ciemała *et al.*, *Nucl. Instrum. Methods A* **608**, 76 (2009).
- [20] J. K. Hartwell and R. J. Gehrke, *Appl. Radiat. Isot.* **63**, 223 (2005).
- [21] M. Balcerzyk, M. Moszynski, and M. Kapusta, *Nucl. Instrum. Methods A* **537**, 50 (2005).
- [22] P. Guss, M. Reed, D. Yuan, A. Reed, and S. Mukhopadhyay, *Nucl. Instrum. Methods A* **608**, 297 (2009).
- [23] A. Oberstedt, R. Billnert, and S. Oberstedt, *Phys. Procedia* **31**, 21 (2012).
- [24] R. Billnert, S. Oberstedt, E. Andreotti, M. Hult, G. Marissens, and A. Oberstedt, *Nucl. Instrum. Methods A* **647**, 94 (2011).
- [25] A. Al-Adili, F.-J. Hamsch, S. Oberstedt, S. Pomp, and Sh. Zeynalov, *Nucl. Instrum. Methods A* **624**, 684 (2010).
- [26] A. Al-Adili, F.-J. Hamsch, R. Bencardino, S. Oberstedt, S. Pomp, and Sh. Zeynalov, *Nucl. Instrum. Methods A* **671**, 103 (2012).
- [27] A. Chyzh, C. Y. Wu, E. Kwan, R. A. Henderson, J. M. Gostic, T. A. Bredeweg, R. C. Haight, A. C. Hayes-Sterbenz, M. Jandel, J. M. O'Donnell, and J. L. Ullmann, *Phys. Rev. C* **85**, 021601 (2012).
- [28] G. Lutter, M. Hult, R. Billnert, A. Oberstedt, S. Oberstedt, E. Andreotti, G. Marissens, U. Rosengård, and F. Tzika, *Nucl. Instrum. Methods A* **703**, 158 (2013).
- [29] A. Oberstedt, S. Oberstedt, R. Billnert, W. Geerts, F.-J. Hamsch, and J. Karlsson, *Nucl. Instrum. Methods A* **668**, 14 (2012).
- [30] G. F. Knoll, *Radiation Detection and Measurement* (Wiley, New York, 2010).
- [31] <http://www.oecd-nea.org/tools/abstract/detail/nea-1525>.
- [32] N. Kornilov, I. Fabry, F.-J. Hamsch, S. Oberstedt, W. Geerts, and V. Fritsch, in *European Commission, Scientific Report 2005, Neutron Physics Unit, EC-JRC IRMM*, edited by S. Oberstedt, EUR 22239 EN, pp. 67–69 (in electronic format only).
- [33] ENDF/B-VII Evaluated Nuclear Data File ZA = 98251, MF = 15, MT = 18 (2011), <http://www.nndc.bnl.gov/exfor/endl00.jsp>.